A NEW DATA REDUCTION SCHEME TO OBTAIN THE MODE II FRACTURE PROPERTIES OF *PINUS PINASTER* WOOD

M.A.L. SILVA*, M.F.S.F. de MOURA, A. B. de MORAIS***, J.J.L. MORAIS***

*** CETAV/UTAD, Department of Mechanical Engineering, Quinta de Prados, 5000-911, Vila Real**
mlsilva@utad.pt, jmorais@utad.pt
**** University of Porto, Faculty of Engineering, Department of Mechanical Engineering and Industrial Management, R. Dr. Roberto Frias, 4200-465 Porto**
mfmoura@fe.up.pt
***** University of Aveiro, Department of Mechanical Engineering, Campus Santiago, 3810-193 Aveiro**
abm@mec.ua.pt

Abstract. In this work a numerical study of the End Notched Flexure (ENF) specimen was performed in order to obtain the mode II critical strain energy released rate (G_{IIc}) of a *Pinus pinaster* wood in the RL crack propagation system. The analysis included interface finite elements and a progressive damage model based on indirect use of Fracture Mechanics.
The difficulties in monitoring the crack length during an experimental ENF test and the inconvenience of performing separate tests in order to obtain the elastic properties are well known. To avoid these problems, a new data reduction scheme based on the equivalent crack concept was proposed and validated. This new data reduction scheme, the Compliance-Based Beam Method (CBBM), does not require crack measurements during ENF tests and additional tests to obtain elastic properties.

1. INTRODUCTION

Nowadays, the structural applications of wood are increasing due to ecological reasons, thus justifying more research on wood fracture behaviour. Consequently, it is essential to obtain the critical strain energy release rate in mode I, II and III. Wood has three orthogonal planes of elastic symmetry: the RL, LT and TR planes, where L, T and R correspond to the longitudinal, tangential and radial directions, respectively. Due to its anisotropy, it is fundamental to characterize six principal systems of crack propagation (RL, TL, RT, LR, LT and TR) [1]. The first letter indicates the direction perpendicular to the crack plane and the second letter designates the direction of the crack propagation.

Actually, there is a considerable interest in the determination of the critical strain energy released rate in mode II (G_{IIc}) in wood. Various test configurations have been proposed, the most important ones being the End Notched Flexure (ENF), the Tapered End Notched Flexure (TENF), the End Loaded Split (ELS) and the Four Point End Notched Flexure (4ENF).

Qiao *et al*. [2] proposed a Tapered End Notched Flexure (TENF) specimen. This specimen does not require crack length measurement during experimental test. However to obtain the value of G_{IIc} it is necessary to know three elastic constants of the beam: Young´s moduli in parallel and transverse directions, and the shear modulus, which should be determined from separate tests. Blackman et al. [3] applied the End Loaded Split (ELS) test to fracture characterization of carbon-fibre-reinforced composite adhesive joints. The authors proposed an effective crack length approach in order to overcome the difficulties related to crack measurement. Recently, a Four Point End Notched Flexure (4ENF) was proposed and examined in the context of mode II fracture characterization of advanced composite materials [4, 5]. Yoshihara [6] used the 4ENF test in order to obtain the *R*-curve on spruce wood specimens. The author verified that a bending failure often occurred near the roller loading the cracked portion before the crack propagation. To prevent bending failure, a specimen with an I-shaped cross-section was prepared. Schuecker *et al*. [7] investigated the effect of friction on the perceived toughness in the ENF and 4ENF tests. The authors considered friction effects on the contacting

surfaces of the initial crack and concluded that this factor induces an error of 2% and 5% on the G_{IIc} value obtained by the ENF and 4ENF tests, respectively.

The ENF test is the most popular test for mode II fracture characterization of wood [8]. Extensive studies have been carried out on analysis, modelling and design of the ENF specimens. A very simplified analytical solution of the ENF specimen based on the simple beam theory was firstly developed by Russell *et al*. [9]. This solution neglects the transverse shear deformation and the crack tip singularity of the specimen and, consequently, underestimates the value of G_{IIc}. Wang *et al*. [10] proposed an additive correction term (χh) to the value of the crack length (a), which accounts for the deformation at the crack tip. In this correction term, h represents half thickness of the specimen and χ is a constant depending on the material elastic properties. Wang and Qiao [11] developed a new analysis for the ENF test. This model is based on the superposition of two sub-problems: an un-cracked beam under three point bending and a skew symmetric beam under shear traction at crack surface. The authors concluded that this model can also be easily extended to analyse other beam type fracture specimens. Silva *et al*. [8, 12] evaluated numerically the performance of the Compliance Calibration Method (CCM) and Corrected Beam Theory (CBT) data reduction schemes in order to obtain the G_{IIc}=f(a) curve, for the RL and TL propagation systems. The authors obtained a good agreement for the CCM method. For the CBT method an acceptable error was obtained for the crack propagation systems studied. However, the referred methodologies have the inconvenient of requiring crack length monitoring during propagation. It is well known that the measurement of the crack length in the ENF test is difficult due to crack propagation without a clear opening. To overcome this problem some solutions have been proposed. Tanaka *et al*. [13] concluded that to extend the stabilized crack propagation range in the ENF test, the test should be conducted under a condition of controlled crack shear displacement (CSD). Silva *et al*.[14] also evaluated the influence of friction on the G_{IIc} value obtained by the ENF test. The authors included the friction effects on the contact surfaces of the initial crack, like Schuecker *et al*. [7], and at the surfaces of propagated crack.

In this work a numerical study of the End Notched Flexure (ENF) test was performed in order to obtain the mode II critical strain energy release rate (G_{IIc}) of a *Pinus pinaster* wood in the RL propagation system. The analysis included interface finite elements and a progressive damage model based on indirect use of Fracture Mechanics. Initially a three-dimensional analysis was performed, in order to evaluate the influence of the energy release rate distribution along the crack front on the G_{IIc} value. A two-dimensional analysis is also carried out to evaluate the influence of Fracture Process Zone (FPZ) on the G_{IIc} value. To avoid the difficulties in monitoring the crack length during an experimental ENF test and the inconvenience of performing separate tests in order to obtain the elastic properties, a new data reduction scheme based on the equivalent crack concept was proposed and validated. The equivalent crack length was incorporated in a Compliance-Based Beam Method (CBBM), which provided accurate values of the mode II critical strain energy release rate, G_{IIc}. This new data reduction scheme (CBBM), does not require crack measurements during ENF tests and additional tests to obtain elastic properties.

2. ANALYSIS

The ENF specimen geometry is presented in figure 1. This test consists of a three point bend configuration, with a lower support rollers and a centre loading pin. The dimensions used for the ENF specimen are: L=230 mm, L_1=250 mm, B=20mm and a_0=162 mm. The initial crack length (a_0) is greater than 0.7L in order to guarantee stable crack propagation [15]. The mechanical properties of wood (*Pinus Pinaster* Ait) are listed in table 1.

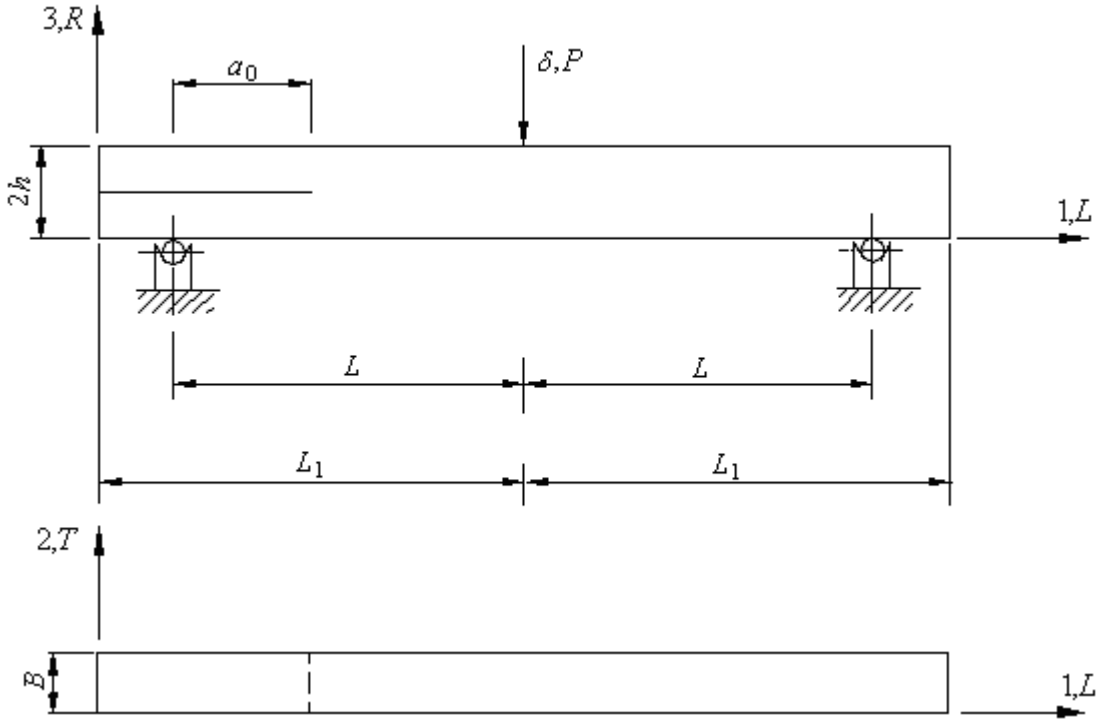

Fig. 1 – Specimen geometry.

E_L (GPa)	E_R (GPa)	E_T (GPa)	υ_{LR}	υ_{TL}	υ_{RT}	G_{LR} (ref.) (GPa)	G_{LT} (ref.) (GPa)	G_{RT} (ref.) (GPa)
15.13	1.91	1.01	0.47	0.51	0.59	1.12	1.04	0.17

σ_L^{ult} (MPa)	σ_R^{ult} (MPa)	σ_T^{ult} (MPa)	τ_{LR}^{ult} (MPa)	τ_{LT}^{ult} (MPa)	G_{Ic} (ref.) (N/mm)	G_{IIc} (ref.) (N/mm)	G_{IIIc} (ref.) (N/mm)
97.46	7.93	4.20	16.0	16.0	0.24	0.63	0.90

Table 1 – Mechanical properties of wood (*Pinus Pinaster* Ait.) [2, 16]

3. FINITE ELEMENT MODELS

Initially a three-dimensional numerical model was constructed within the commercial software ABAQUS® using three-dimensional 8 node brick elements and previously developed 8 node interface finite elements [17, 18]. The finite element mesh used had 29750 brick elements and 5220 interface finite elements (Figure 2). In the initial crack faces contact conditions were imposed to prevent interpenetration of the cracked parts. The interface finite elements were placed at the mid-plane (h) of the uncracked region. The numerical analyses were performed considering nonlinear geometrical behaviour. A loading displacement was applied incrementally at the mid-span of the specimen, considering a very small value of the increment (0.01 % of the total displacement) to ensure a smooth propagation process. The *P-δ-a* values obtained were used to estimate G_{IIc} by the Compliance Calibration Method (CCM), Corrected Beam Theory (CBT) and Compliance-Based Beam Method (CBBM).

The energy release rate distribution along the width of the specimen was obtained considering an adaptation of the usual Virtual Crack Closure Technique (VCCT). In this case, stresses and relative displacements at the nodal points of the interface elements are used in order to obtain,

$$G_{\mathrm{I}} = \frac{\sigma_{j3}(w_{k\mathrm{t}} - w_{k\mathrm{b}})}{2}$$
$$G_{\mathrm{II}} = \frac{\tau_{j31}(u_{k\mathrm{t}} - u_{k\mathrm{t}})}{2} \quad (1)$$
$$G_{\mathrm{III}} = \frac{\tau_{j32}(v_{k\mathrm{t}} - v_{k\mathrm{t}})}{2}$$

where σ_{j3}, τ_{j31} and τ_{j32} denote the nodal stresses at the delamination front. The corresponding displacements behind the delamination at the top face (node kt) are denoted as $u_{k\mathrm{t}}$, $v_{k\mathrm{t}}$ and $w_{k\mathrm{t}}$ and at the bottom face (node kb) are denoted $u_{k\mathrm{b}}$, $v_{k\mathrm{b}}$ and $w_{k\mathrm{b}}$, as shown in figure 3. The principal advantage of using this approach is that it can be performed in a first loading step of more complete crack propagation analysis. As expected, both forms of VCCT gave identical energy release rate distribution along the crack front.

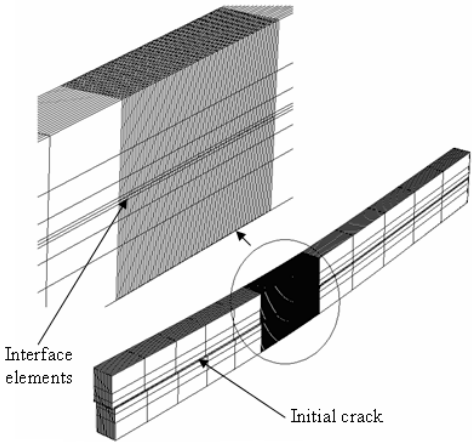

Fig. 2 – Mesh of three-dimensional finite element model of ENF specimen.

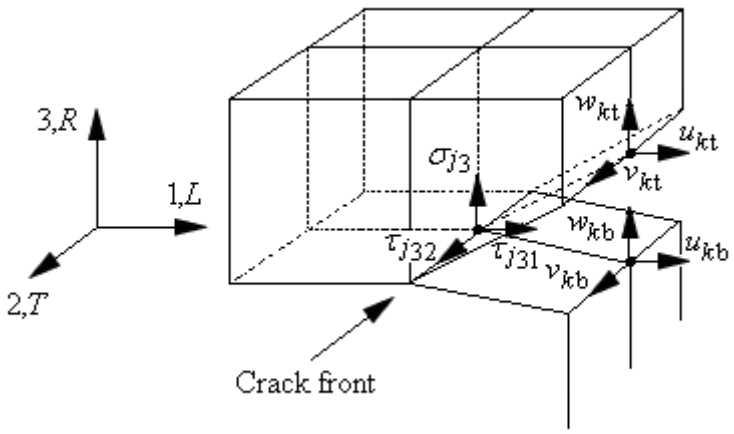

Fig. 3 – Scheme of the local nodes used for the VCCT.

In order to validate a 2D approach, a two-dimensional finite element model with 8-node plane strain elements and 6-node interface finite elements were constructed (Figure 4). The used mesh had 2750 brick elements and 164 interface finite elements. Detail 1 corresponds to the initial crack, where contact conditions were imposed to prevent interpenetration of the cracked parts. The interface finite elements are placed at the mid-plane of the uncracked region (represented by diagonal crosses in the detail 2, of figure 4). Contacting surfaces were also considered between the specimen and the supports/actuator, which were defined as rigid bodies. The analyses were performed considering plane strain conditions and nonlinear geometrical behaviour.

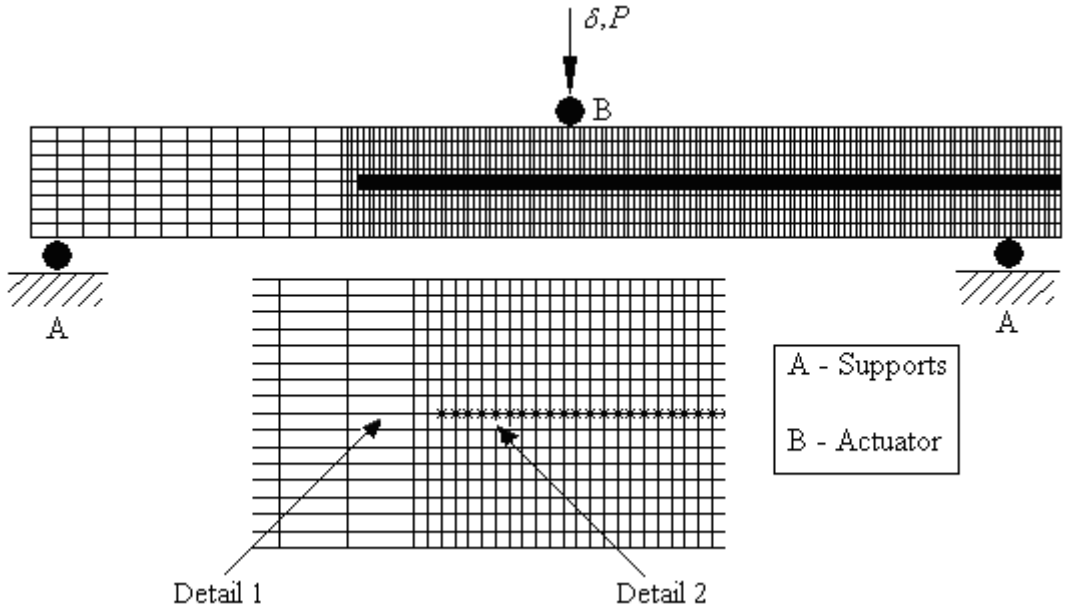

Fig. 4 –Two-dimensional finite element model of ENF test.

4. TWO-DIMENSIONAL ANALYSIS VALIDATION

The mode I energy release rate was found to be negligible. Figure 5 shows the predominance of mode II along the width of the specimen. The average of mode II component represents 99.8% of total energy release rate. The mode III component (Figure 6) is about 1.14% at the specimen edges, although its average is less than 0.2 % of total energy release rate.

During the test simulation the values of P-δ-a were registered. Compliance ($C=\delta/P$) versus crack length (a) data were fitted by a third order polynomial,

$$C = C_1 a^3 + C_0 \tag{2}$$

The most commonly used technique to obtain G_{IIc} is the Compliance Calibration Method (CCM). The fundamental equation used for this method is given by [1],

$$G_{IIc} = \frac{P^2}{2B}\frac{dC}{da} \tag{3}$$

where P is the total applied load and B is the width of the specimen. Substituting equation (2) in equation (3) leads to

$$G_{IIc} = \frac{P^2}{2B}\left(3\,C_1\,a^2\right) \tag{4}$$

In figure 7 a good agreement between the numerical and the reference value of G_{IIc} can be observed. The behaviour of G_{IIc}=f(a) curve is similar considering a two-dimensional or a three-dimensional element finite models. Figure 8 shows the good agreement between the P-δ curves obtained considering 2D and 3D analysis. Consequently these results validate the use of a 2D approach, with significant advantages in terms of computing effort.

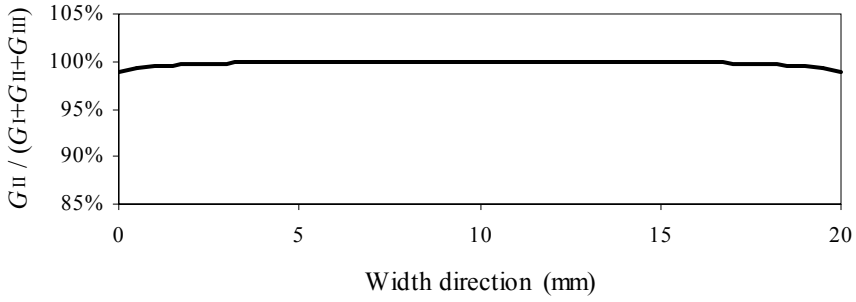

Fig. 5 – Distribution of $G_{II}/(G_I + G_{II} + G_{III})$ along the width of ENF specimens.

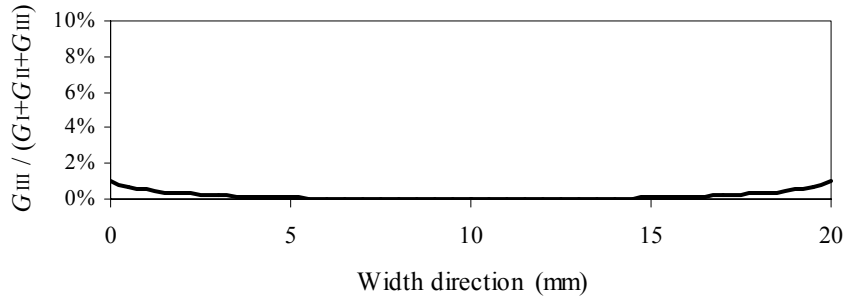

Fig. 6 – Distribution of $G_{III}/(G_I + G_{II} + G_{III})$ along the width of ENF specimens.

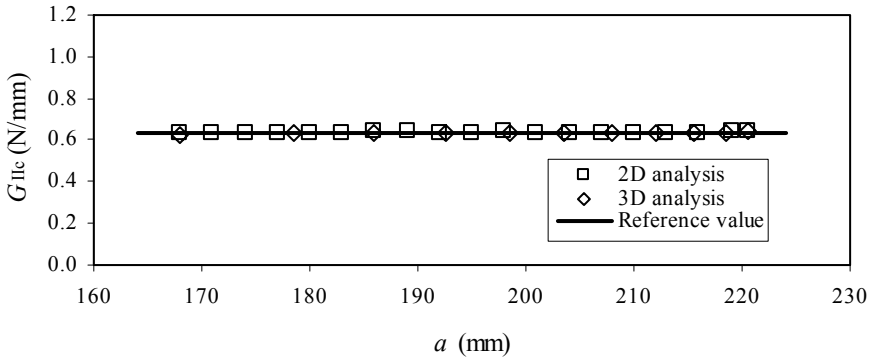

Fig. 7 – Comparison between the R-curves obtained from 2D and 3D analysis.

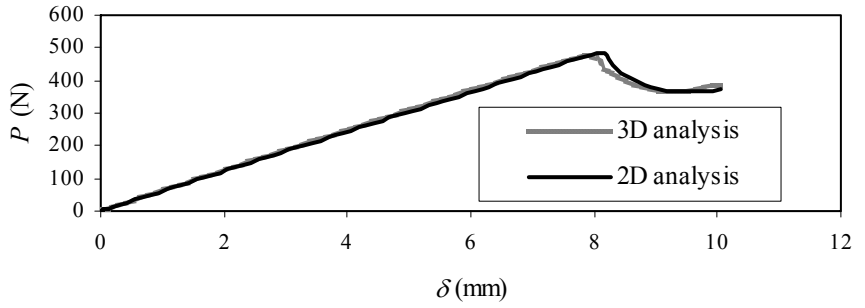

Fig. 8 – Comparison between P-δ curves obtained from 2D and 3D analysis.

5. G_{IIC} PREDICTION

Three different data reduction schemes were used in order to evaluate their performance: the Compliance Calibration Method (CCM), the Corrected Beam Theory (CBT) and the Compliance-Based Beam Method (CBBM). The CCM was applied considering equation (4). The Corrected Beam Theory (CBT) is based on the following equation

$$G_{\mathrm{IIc}} = \frac{9P^2a^2}{16B^2E_f h^3}\frac{F}{N}f_v \tag{5}$$

where F and N are correction factors to account for large displacement effects, for the moment arm and for the compliance, respectively. The term f_v comprises the effect of transverse shear. As it can be observed in figure 9, good agreement with the inputted value is obtained. However the CBT slightly underestimates the G_{IIc} value. This phenomenon can be explained by the development of a Fracture Process Zone (FPZ), which corresponds to a non-negligible region of damaged material, ahead of the crack tip [8]. Although the G_{IIc} values obtained by the CCM (figure 7) and CBT (figure 9) present good agreement with the G_{IIc} (ref) value, these methodologies require crack monitoring during the ENF test, which is disadvantageous.

To overcome these problems, a new data reduction scheme based on the equivalent crack concept was proposed and validated. This new data reduction scheme (CBBM), does not require crack measurements during ENF tests and additional tests to obtain elastic properties. The strain energy of the ENF specimen due to bending, and including the shear effects, is given by

$$U = \int_0^{2L}\frac{M_f^2}{2E_f I}dx + \int_0^{2L}\int_{-h}^{h}\frac{\tau^2}{2G_{\mathrm{LR}}}B\,dy\,dx \tag{6}$$

where M_f represents the bending moment and I represents the second moment of area. The value of τ can be obtained by

$$\tau = \frac{3}{2}\frac{V_i}{A_i}\left(1-\frac{y^2}{{c_i}^2}\right) \tag{7}$$

where A_i represent the cross-section area, c_i the half-thickness of the beam and V_i the transverse load of the i segment ($0\le x\le a$, $a\le x\le L$ or $L\le x\le 2L$). Using the Castigliano theorem one obtains the displacement of loading point

$$\delta = \frac{dU}{dP} = \frac{P\left(3a^3+2L^3\right)}{12E_f I} + \frac{3PL}{5G_{\mathrm{LR}}A} \tag{8}$$

with A=2Bh. The flexural modulus of the ENF specimen can be obtained from equation (8) using the initial compliance (C_0)

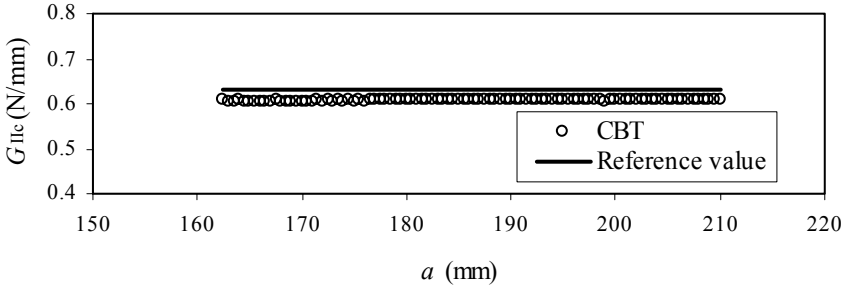

Fig. 9 – G_{IIc}=f(a) curve obtained by CBT

$$E_f = \frac{3a_0^3 + 2L^3}{12\,I}\left(C_0 - \frac{3L}{5\,G_{\mathrm{LR}}\,A}\right)^{-1} \tag{9}$$

During crack propagation a correction of the real crack length is considered in the compliance (equation (8)) to include the FZP effect

$$C = \frac{3(a + \Delta a_{\mathrm{FPZ}})^3 + 2L^3}{12E_f\,I} + \frac{3L}{5G_{\mathrm{LR}}\,A} \tag{10}$$

and consequently,

$$a_{\mathrm{eq}} = a + \Delta a_{\mathrm{FPZ}} = \left[\frac{C_{\mathrm{corr}}}{C_{0\,\mathrm{corr}}}a_0^3 + \frac{2}{3}\left(\frac{C_{\mathrm{corr}}}{C_{0\,\mathrm{corr}}} - 1\right)L^3\right]^{1/3} \tag{11}$$

where C_{corr} is obtained by

$$C_{\mathrm{corr}} = C - \frac{3L}{5\,G_{\mathrm{LR}}\,A} \tag{12}$$

Substituting equation (11) in equation (5), without the corrections factors, gives

$$G_{\mathrm{IIc}} = \frac{9P^2}{16B^2E_f h^3}\left[\frac{C_{\mathrm{corr}}}{C_{0\,\mathrm{corr}}}a_0^3 + \frac{2}{3}\left(\frac{C_{\mathrm{corr}}}{C_{0\,\mathrm{corr}}} - 1\right)L^3\right]^{2/3}. \tag{13}$$

From equation (13) it can be concluded that the G_{IIc} value obtained by the Compliance-Based Beam Method (CBBM) does not depend explicitly on the crack length value (a). Thus, during an experimental test it is only necessary to register the values of the applied load (P) and displacement (δ). Moreover, as the presence of the FPZ influences the compliance, its effects are included in this approach. On the other hand, CBBM does not depend on the flexural modulus, which can be considered an important advantage. In fact, due to the wood heterogeneity, the flexural modulus (E_f) is specimen dependent. By using this methodology, it is not necessary to perform additional tests to obtain this property. To assess the influence of G_{LR} on G_{IIc}, a variation of this property around its reference value $400 \leq G_{\mathrm{LR\,(ref)}} \leq 1900$ MPa was performed (see figure 10). As it can be seen, this material property does not have significant influence on the G_{IIc} value. A good agreement between the numerical (CBBM derived) and the reference value of G_{IIc} was obtained (Figure 11). Table 2 presents a comparison between the average G_{IIc} values obtained from all data reduction methods (CCM, CBT and CBBM) and the reference value.

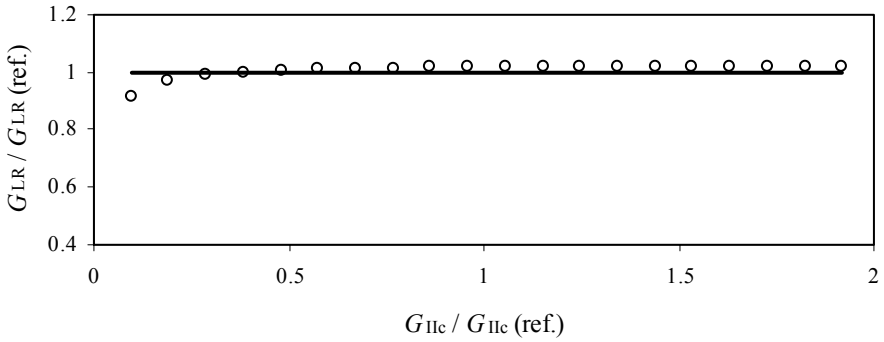

Fig. 10 – Influence of G_{LR} on G_{IIc}.

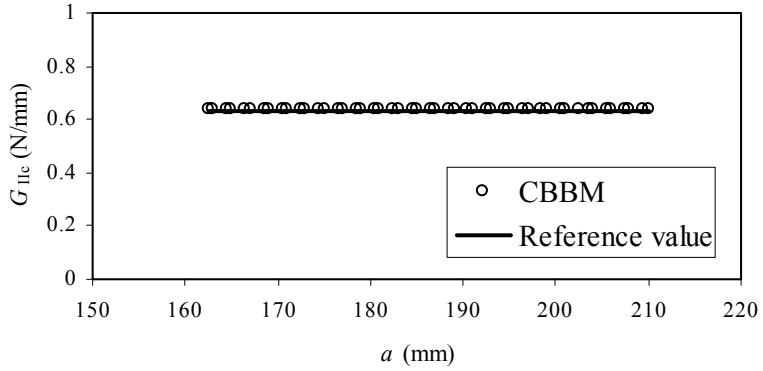

Fig. 11 – G_{IIc}=f(a) curve obtained by CBBM.

		CCM	CBT	CBBM
Reference value G_{IIc} (ref.)=0.63 (N/mm)	G_{IIc} (N/mm)	0. 632	0.611	0.640
	Error (%)	0.39	-3.11	1.56
	St. Dev.[a] (%)	1.01	0.34	0.25

[a] The standard deviation (St. Dev) is calculated relatively the average value of the G_{IIc}.

Table 2 – Comparison between the G_{IIc} average values, obtained by the CCM, CBT and CBBM, and the reference value for the RL crack propagation system.

6. CONCLUSIONS

In this work a numerical study of the End Notched Flexure (ENF) specimen was performed in order to evaluate the accuracy of several data reduction schemes to obtain G_{IIc} of a *Pinus pinaster* wood in the RL crack propagation system. The numerical models included interface finite elements and a progressive damage model to simulate crack propagation. Initially a three-dimensional numerical VCCT analysis was performed in order to obtain the energy release rate distribution along the width of the specimen. From this study we concluded that an almost pure mode II exists at the crack front. Considering the computational effort a two-dimensional analysis was proposed and validated to obtain the G_{IIc} value.

The CCM showed good agreement with the reference value of G_{IIc}. The CBT slightly underestimated G_{IIc} which is explained by the FPZ not being accounted in this method. Finally, a Compliance-Based Beam Method (CBBM) was developed, which includes the FPZ effects ahead of the crack tip. This data reduction scheme does not require crack measurement during propagation and additional experimental tests to measure the elastic properties. Good agreement between the predicted and inputted values of G_{IIc} was obtained with this methodology.

7. ACKNOWLEDGMENTS

The authors thankful the Portuguese Foundation for Science and Technology (FCT, research project POCTI/EME/45573/2002) for supporting the work here present.

8. REFERENCES

[1] Smith, I., et al, "Fracture and Fatigue in Wood", John Wiley & Sons ltd, 2003, England.

[2] Qiao, P., Wang, J., Davalos, J.F., "Analysis of tapered ENF specimen and characterization of bonded interface fracture under mode II loading", Int J Solids Struct, 40, 1865-1884 (2003).

[3] Blackman, B.R.K., Kinloch, A.J., Paraschi, M., "The determination of mode II adhesive fracture resistence, G_{IIc}, of structural adhesive joints: an effective crack length approach", Eng Fract Mech, 72, 877-897 (2005).

[4] Martin, R.H., Davidson, B.D., "Mode II fracture toughness evaluation using four point bend, end notched flexure test" Plast. Rubber Compos, 28(8), 401-406 (1999).

[5] Schuecker, C., Davidson, B.D., "Evaluation of accuracy of the four point bend end-notched flexure test for mode II delamination toughness determination", Composites Science Technology, 60, 2134-2146 (2000).

[6] Yoshiara, H., "Mode II R-curve of wood measured by 4-ENF test", Eng Fract Mech, 71, 2065-2077 (2004).

[7] Schuecker, C. and Davidson, B.D., "Effect of friction on the perceived mode II delamination toughness from three and four point bend end notched flexure tests", ASTM STP 1383, pp. 334-344 (2000).

[8] Silva, M.A.L., de Moura, M.F.S.F. and Morais, J.J.L., "Numerical Analysis of the ENF Test for Mode II Wood Fracture" *in press* on Composites Part A, 2005.

[9] Russell, A.J., et al, "Factors affecting the interlaminar fracture energy of graphite/epoxy laminates", In: Proceedings of ICCM4, 1982, Tokyo, pp. 279-286.

[10] Wang, Y. and Williams J.G., "Corrections for Mode II Fracture Toughness Specimens of Composite Materials", Composites Science & Technology, 43, 251-256 (1992).

[11] Wang, J. and Qiao P., "Novel beam analysis of end notched flexure specimen for mode-II fracture", Eng Fract Mech, 71, 219-231 (2004).

[12] Silva, M.A.L., et al, "Análise por elementos finitos do ensaio ENF (End Notched Flexure) para a determinação das propriedades de fractura da madeira, Pinus Pinaster.Ait.", In: Proceedings of Congreso de Métodos Numéricos en Ingeniéria 2005, Granada, pp. 279.

[13] Tanaka, K., Kageyama, K., Hojo, M., "Prestandardization study on mode II interlaminar fracture toughness test for CFRP in Japan", Composites, 26(4), 243-255 (1995).

[14] Silva, M.A.L., et al, "Numerical analysis of the ENF test on the mode II fracture of wood", In: Proceedings of the III conference of ESWM 2004, Vila Real, pp. 77-84.

[15] Kageyama, K., Kikuchi, M., Yanagisawa, N., "Stabilized end notched flexure test:characterization of mode II interlaminar crack growth", ASTM STP 1110, pp. 210-225 (1991).

[16] Caumes, P., "Rupture d´un materiau anisotropic en conditions polymodales (Le bois) ", Thèse Docteur, Université de Bordeaux I, 1987.

[17] Gonçalves, J.P.M., de Moura, M.F.S.F., Castro, P.M.S.T., Marques, A.T., "Interface element including point-to-surface constraints for three dimensional problems with damage propagation", Engineering Computations, 17, 28-47 (2000).

[18] de Moura, M.F.S.F., Gonçalves, J.P.M., Marques, A.T., Castro, P.M.S.T., "Modeling compression failure after low velocity impact on laminated composites using interface elements", Journal of Composite Materials, 31, 1462-1479 (1997).